# Effect of microwave and thermal co-pyrolysis of low rank coal and pine wood on product distributions and char structure

# Effect of Microwave and Thermal Co-pyrolysis of Low Rank Coal and Pine Wood on Product Distributions and Char Structure

Victor Abdelsayed[1,2,*], Candice Ellison[1,2], Anna Trubetskaya[3], Mark Smith[1], Dushyant Shekhawat[1]

[1]National Energy Technology Laboratory, 3610 Collins Ferry Road, Morgantown, WV 26507, USA

[2]Leidos Research Support Team, 3610 Collins Ferry Road, Morgantown, WV 26507, USA

[3]Department of Chemical Sciences, University of Limerick, Castletroy, Ireland

**ABSTRACT**

Direct conversion of a low-rank coal into valuable chemicals or improving its char's coking value became very demanding goals in coal utilization strategies. In this work, the co-pyrolysis of a low-rank lignite coal and pine wood sawdust biomass blended at a 3:1 coal-to-biomass ratio was investigated along with original coal and biomass samples by microwave assisted and conventional thermal methods at 550℃ under nitrogen and ambient pressure. The carbon structure and its reactivity in generated chars and the product distributions were greatly affected by the applied heating mechanism and the presence of biomass during coal pyrolysis. High gas and low tar yields were observed for all microwave chars in comparison to thermal chars, regardless of composition. The addition of biomass to coal increased the tar yield under both methods and to a higher extent under the microwave. This agrees with the high gas yield and high aromatic-to-aliphatic fraction observed under the microwave and the presence of biomass. The high O/C ratio and low fixed carbon content in a biomass structure relative to coal affect the product distribution during microwave pyrolysis. This could selectively heat the biomass in the sample, remove its polar groups, and convert it into an efficient microwave absorber biochar that can decompose coal efficiently during co-pyrolysis. The aromatic carbon stacking and its ordering in the generated chars were investigated by powder X-ray diffraction, Raman spectroscopy, dielectric property measurements, and electron spin resonance techniques. A synergistic effect was observed upon biomass addition during microwave coal pyrolysis. Electron spin resonance spectroscopy revealed that the microwave coal/biomass char is the most stable char with the lowest free radical concentration. This agrees with the highest $I_G/I_{all}$ band area ratio calculated from Raman analysis revealing a more graphitic nature for carbon in this char. Similarly, the dielectric properties confirmed that the addition of biomass to coal under the microwave has the highest loss tangent, indicating a high graphitic nature compared to pure biochar or coal char.

*Keywords:*

*Lignite coal, microwave, co-pyrolysis, biomass, char characteristics, dielectric, radical concentration, pine wood, ESR*

*Corresponding author. Tel:+13042855273; fax: +13042854850.

E-mail address: Victor.Abdel-Sayed@netl.doe.gov

## 1. Introduction

Coal remains a large part of the global energy economy, making up 18% of all energy production in the United States based on 2017 estimates.1 Although anthracitic and bituminous coals are used directly for metallurgy or combustion in coal-fired plants, utilization of low-rank coals (including lignite and sub-bituminous) is not economical due to their low calorific value, high moisture content, and high ash content. In the United States, over half (55%) of all produced coal is low rank (2017 estimate), providing an abundant, low cost feedstock for conversion to high-value chemicals.[1] Several coal-to-chemicals pathways exist, including pyrolysis, gasification, and liquefaction; of these, pyrolysis is the only single-step conversion process that is carried out at atmospheric pressure. Pyrolysis is considered the initial treatment step for gasification and combustion, making it a fundamental process for further study. Co-utilization of the lignite coal with the biomass, another abundant, low-cost feedstock, has been reported to reduce $CO_2$, $SO_x$, and $NO_x$ emissions compared to pure coal, providing a suitable short term strategy for clean fossil energy utilization.[2] Although many researchers have focused their work on biomass addition to lower coal emissions, little has been done to improve the coking nature of produced chars during co-pyrolysis, which suffer from low thermal stability and heating value, and still cannot be used in the metallurgical or ferroalloy industries. This is in part because of the complex nature of these fuels and lack of adequate mechanistic studies and comprehensive understanding of free radical formation during co-pyrolysis. Utilization of these hybrid chars in metallurgical or ferroalloy industries should lower the carbon foot print used for met coke. Many studies have investigated the pyrolysis behavior of low-rank coal[3] or lignocellulosic biomass4 individually as well as co-pyrolysis of coal and biomass mixed feedstocks.[5] Devolatilization kinetics of biomass and coal differs due to differences in the bond energies of the molecules making up each material.6 In general, biomass decomposition initiates at lower temperatures and coal decomposition initiates at higher temperatures, which is attributed to differences in the macromolecular structure of the parent material. Biomass macromolecules are linked by weak ether bonds (C-O-C), whereas coal is made up of condensed ring systems linked by strong aromatic bonds (C=C) requiring greater energy input to cleave.[7] Most studies regarding the interaction of coal and biomass mixed feedstocks during co-pyrolysis have observed non-additive (synergistic) product distributions.[5b,c,8] Synergy is typically reported at certain intermediate temperatures during co-pyrolysis at which devolatilization of both feedstocks occurs at the same time and is especially evident when the coal fraction is of low rank.[5c,6b] Although a tremendous work has been conducted on co-pyrolysis of coal and biomass feedstocks, there is no clear interaction mechanism to explain the observed synergistic effects during their co-pyrolysis. Some investigations attributed synergistic effects during coal and biomass co-pyrolysis to OH and H radicals from the biomass, which facilitate the decomposition of lignite as well as secondary volatile reactions with the catalytically active mineral phases within the coal and biomass char.[8,9] Others, like Vuthaluru,[10] reported that no synergy effects were observed in activation energy during co-pyrolysis. Most of the pyrolysis work has been conducted by using thermal heating sources such as electric and gas heater.[11] Generally, carbon is a good microwave absorber due to its high conductive losses under microwave polarization and can be easily heated under the microwave radiation.[12] Therefore, utilizing microwaves to heat biomass particles could be a more promising technique than thermal pyrolysis because the use of microwaves intensifies pyrolysis reactions and, thus, increases overall process efficiency.[3a,13] Under thermal heating, fuels are heated by conduction and convection from the reactor walls producing a thermal gradient with greater temperatures near the reactor walls and lower temperatures in the center of the material volume. The previous studies showed that a higher corn stover to brown coal ratio resulted in a greater oil yield, whereas a greater heat treatment temperature increased the oil yield in brown coal and coal/corn mixtures co-pyrolysis.[14] In addition, the results showed that the $CO_2$ yield is relatively high and the $H_2$ yield is relatively low in thermal pyrolysis of coal, whereas the microwave pyrolysis of coal and biomass blends generated a significantly greater fraction of $H_2$, CO, and $CH_4$.[15] The optimal microwave powers and heat treatment temperatures were mainly in the range of 300−1500 W and 260−877 °C for the bio-oil production from co-pyrolysis of macroalgae and lignocellulosic feedstock.16 The co-pyrolysis of macroalgae and lignocellulosic biomass gave the maximum pyrolysis oil at a heat treatment temperature of 450 °C and a heating rate of 20 K min$^{-1}$ with 80% mass of rice husk in the mixture.[17] However, little is known about structure−property relationships of the product governing the radical formation during co-pyrolysis of blends in both thermal and microwave-assisted pyrolysis processes. Thus, it is important for the industrial use of coal and biomass blends to understand how the structural properties of chars from co-pyrolysis are related to the radical concentration and composition to maximize the bio-oil yields. Pyrolytic chars exhibit complex structural characteristics and with little or no additional processing may be utilized as feedstocks for value-added products, e.g., activated carbon,[18] catalyst supports,[19] soil amendment,[20] or metallurgy.[21] As such, it is important to characterize the structure and composition of chars generated by pyrolysis to better guide their application. Pyrolysis of mixed feedstocks could produce chars with unique properties compared to chars generated from a single feedstock. In a recent study, Wu et al. carried out co-pyrolysis of wheat straw with two ranks of coal : anthracite and bituminous.[22] In both cases, wheat straw promoted an increase in a specific surface area of the generated chars; however, an increase in the wheat straw mass ratio reduced the carbon ordering and uniformity of micropores in the char.[22] In a study on co-pyrolysis of corn stover and Pennsylvania coal blends at different temperatures, the authors describe a synergistic relationship for the porosity development of the chars.[6a] At low temperatures, the char surface area and microporosity are not affected by the blend ratio; however, with the increasing pyrolysis temperature, the addition of biomass increases the microporosity of the reacted chars.[6a] As char properties from pyrolysis of mixed feedstocks are difficult to predict owing to the non-additive nature of co-pyrolysis, it is important to characterize pyrolytic chars to gain an understanding of their structural and compositional properties to help guide their application. In addition, co-pyrolysis of coal and biomass can lower the non-benign emissions and formation of free radicals and particulates into the environment. It also helps in gaining a better understanding of the interaction between coal and biomass toward the formation of chars and chemical products with tunable properties.[23] Despite the existence of enormous results on individual pyrolysis of coal, biomass and lignocellulosic components, the co-pyrolysis of biomass and coal with respect to product properties and the radical formation has received little attention. Many investigations have used electron spin resonance (ESR) spectroscopy to study the chemical structure of free radicals and its concentrations in pyrolysis products.[24] A number of ESR studies have been reported in which there was a dramatic increase in the free radical concentration when coals were heated above 400°C.[25] Although direct characterization of biomass and coal co-pyrolysis using electron spin resonance spectroscopy has not been reported, the free radical formation was investigated in several studies.[26] The results of previous studies at high-temperature pyrolysis indicated that the biomass major constituents (cellulose, hemicellulose, lignin) had a minor effect on remaining radical concentrations compared to potassium and silica contents.[26b] The concentration of hydroxyl groups in the macromolecular structure of biomass is higher than that in the coal. Thus, during biomass pyrolysis, the high concentration of small free radicals of OH and H, found in its volatiles, can strongly combine with other free radicals as well as penetrate into the char matrix while in contact with the products from coal pyrolysis.[27] The thermal decomposition reactions for coal usually generate large free radicals, which could combine with small biomass free radicals and lead into its stabilization. This could reduce the occurrence of secondary cracking reactions during pyrolysis and lead to the formation of stable fragments that escape the reaction zone in the form of volatiles. Thus, the addition of biomass to coal during pyrolysis could improve the devolatization rate and increase the tar yield.[28] The knowledge about remaining free radicals in the char from co-pyrolysis of coal and biomass can help to understand the role of free radicals trapped in the solid matrix on the biomass-coal cross-linking/depolymerization and, thus, on the chemical structure of pyrolysis products. Despite the ubiquity of free radicals, the structure and yields of radicals in co-pyrolysis of biomass and coal have not been well understood and well characterized. Throughout the course of this work, we have attempted to gain an understanding of the chemical structure and yields of radicals from microwave-assisted and thermal co-pyrolysis of coal and biomass blends. The objective of the present work was to characterize experimentally the char structure and remaining free radicals in the chars from co-pyrolysis of biomass and coal blends. The knowledge about remaining free radicals will help to relate the char structural changes to the role of free radicals trapped in the solid matrix on the crosslinking/depolymerization of the biomass and coal blends. A primary emphasis of the present study was placed on the influence of the pyrolysis process and the synergistic effect of biomass and coal blends on the radical formation. A secondary emphasis was placed on the microwave-specific effect on the product yield distribution and char structure evolution during pyrolysis to optimize co-pyrolysis reaction conditions to target desired products.

## 2 Experimental

### *2.1 Raw materials*

Fuel feedstocks of pulverized Mississippi coal, a low rank lignite coal, and Yellow pine sawdust, a biomass wood pellets, were supplied by National Carbon Capture Center (NCCC) through Southern Company. The coal powder was further homogenized by ball milling, then pressed and sieved between 300 and 600 μm particle sizes. Wood pellets were ground using a high-speed rotary mill before being sieved into similar particle size fractions. Table1 below shows the proximate, ultimate and ash analysis for coal and biomass samples used in this study.

Table 1. Ultimate, proximate and ash composition of lignite coal and wood pellets

| Sample | | Lignite Coal | Pine Biomass |
|---|---|---|---|
| Proximate analysis/ (wt%, dry basis) | Volatile | 43.76 | 85.19 |
| | Fixed carbon | 30.53 | 13.40 |
| | Ash | 25.71 | 1.42 |
| Ultimate analysis/ (wt%, dry basis) | C | 51.75 | 53.20 |
| | H | 3.57 | 6.24 |
| | N | 1.27 | 0.12 |
| | S | 0.73 | 0.02 |
| | O[a] | 16.97 | 39.00 |

[a] by difference; O (wt%) = 100-C-H-N-S-Ash

| Sample | Al | Si | Ca | Ba | Fe | Mg | Mn | P | K | Na | Sr | S | Ti |
|---|---|---|---|---|---|---|---|---|---|---|---|---|---|
| Lignite Coal | 18.80 | 45.30 | 19.00 | 0.17 | 3.74 | 3.57 | 0.34 | 0.07 | 1.05 | 0.47 | 0.41 | 5.61 | 1.15 |
| Pine Biomass | 13.80 | 37.80 | 21.20 | 0.21 | 4.15 | 6.12 | 2.57 | 1.74 | 4.06 | 1.07 | 0.30 | 5.50 | 0.77 |

### *2.2 Pyrolysis*

The pyrolysis studies were carried out under two different methods: microwave-assisted and conventional thermal heating methods. For microwave pyrolysis, a pulsed fixed frequency (2.45 GHz) microwave reactor from Sairem (model: GMP20K) with a 2-kW magnetron was used. A fixed-bed quartz tube reactor with a one inch (ID) diameter was placed inside a 500 W single mode microwave cavity. The sample temperature was monitored during the reaction from a small port in the microwave cavity using an IR pyrometer from Micro-Epsilon, model CTLM3. The pyrometer temperature sensitivity was between 200 °C and 1500 °C. By adjusting the microwave duty cycle, the reaction temperature can be controlled. By controlling the duration of cooling and heating times of microwave pulses, the coal/biomass bed can be maintained within an acceptable temperature window. All pyrolysis experiments were conducted at 550 °C.

An electric furnace fixed-bed reactor was used to conduct conventional thermal pyrolysis. First, the temperature of the quartz reactor was ramped and maintained at 550 °C under $N_2$ gas flow. Once the reactor equilibrates, the sample was quickly dropped using a feeder into the reactor hot zone.

Typically, 10g of raw lignite coal, ground pine or a mixture of ground pine and coal (25 wt.% pine) was loaded into the reactor and pyrolyzed under pure $N_2$ (UHP, 99.999 %) for two hours. The total gas flow was fixed at 300 sccm, and the experiments were operated under atmospheric pressure. The generated chars were given these abbreviations: *C*, *B* and *CB*, to stand for coal, biomass, and their mixed samples, respectively. The pyrolysis method was given as: *MW* or *Conv*, to indicate whether the char was prepared under microwave or conventional thermal method. For example, *CB-MW* sample is for coal and biomass blended char generated under microwave pyrolysis. The experimental setup used for microwave-assisted pyrolysis of coal/biomass samples is given in Figure 1 below.

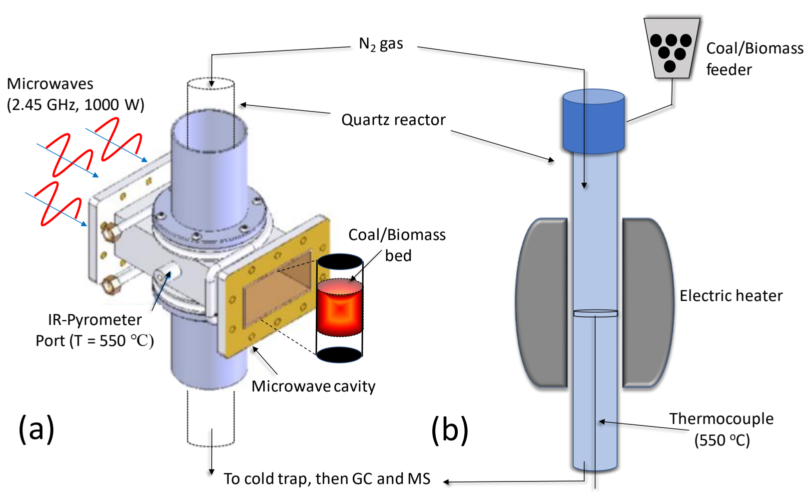

Figure 1. Experimental setup used for (a) microwave-assisted and (b) thermal pyrolysis of coal/biomass samples at 550 °C under $N_2$ at ambient pressure.

*2.3 Analysis of products*

Oil and waxy tars were separated from gases exiting reactor using two cold traps maintained below freezing point temperature (-10 °C) and at room temperature (25 °C), respectively. Remaining gases (hydrogen, nitrogen, carbon monoxide, carbon dioxide and methane) and some light hydrocarbons (acetylene, ethylene, ethane, propylene, 1,3-butadiene, benzene and toluene) were analyzed online using a mass spectrometer (Prima BT from Thermo Fisher Scientific) and a 4-channel micro gas chromatograph (μGC -3000A from Agilent).

Pyrolysis product yields were calculated using the following equations:

$$Y_{tar} = 100 \times \frac{wt.of\ oil\ and\ waxy\ tars}{initial\ wt.of\ sample} \quad (1)$$

$$Y_{char} = 100 \times \frac{wt.of\ char}{initial\ wt.of\ sample} \quad (2)$$

$$Y_{gas} = 100 - (Y_{tar} + Y_{char}) \quad (3)$$

*2.4 Char characterizations*

*2.4.1 Surface area*

Surface area analysis were measured using Micromeritics ASAP-2020 unit at 77 K and by using $N_2$ as the adsorption gas. Char samples were first degassed under vacuum and at 300 °C for 10 hours to clean the char surfaces of any pre-adsorbed gases and moisture before measuring its surface properties. Brunauer-Emmett-Teller (BET) model [29] was used to calculate the surface area using adsorption isotherms data. The pore size distributions (PSD) of chars were calculated from the desorption isotherm using Barrett-Joyner-Halenda (BJH) model. The *t*-plot analysis were used to calculate the micropore volumes and areas of chars [30].

*2.4.2 Scanning electron microscopy*

The morphologies of chars prepared under microwave and thermal pyrolysis methods were tested using scanning electron microscope (JEOL FE-7600). A very thin layer of char powder was first placed on a carbon double-sided tape supported on a copper stud before it was placed inside the microscope. The SEM images were collected under an acceleration voltage of 15 KV and a working distance of 39 mm.

*2.4.3 Powder X-ray diffraction*

The X-ray diffraction of collected chars were measured using a PANalytical X'pert Pro (PW3040) unit equipped with a Cu tube ($K_{\alpha}$ radiation $\lambda$=0.1541 nm) maintained at 45 kV, 40 mA). A Si sample holder with zero-diffraction was used during all measurements. The char samples were scanned between $2\theta$ = 10 ° to 70 ° with a scan speed of 0.026°/s. Highscore Plus software was used in peak identification using X-ray diffraction database (ICDD).

*2.4.4 Raman analysis*

Raman spectroscopy was utilized to examine carbon structures in collected chars. The char spectra were collected at room temperature and ambient pressure using a Jobin Yvon Labram HR Evolution spectrometer. A few milligrams of char sample were first placed under a microscope equipped with a 100 X objective lens. A 25mW laser beam (532 nm, Nd:YAG) was focused on the sample to excite it. The back-scattered Raman signal was collected using a CCD detector and a 1800 gratings/mm. The first order bands region was recorded between 800 $cm^{-1}$ and 2000 $cm^{-1}$. Each char sample was measured at least three different times on different spots to insure reproducibility. OriginLab 2018b software was used to deconvolute the collected Raman spectra and determine the corresponding spectral parameters. The modified Knight formula [31] was used to calculate the carbon microcrystalline planner size ($L_a$) and is given below in equation 4:

$$L_a = \frac{C_o + C_1\lambda_L}{I_D/I_G} \quad (4)$$

Where $C_o$ and $C_1$ are constants that depend on the excitation laser wavelength ($\lambda_L$). So between 400 nm and 700 nm excitation wavelength, $C_o$ is equal to 12.6 nm and $C_1$ is equal to 0.033 nm. The ratio $I_D/I_G$ is the band area ratio between $D_1$ and G bands.

### *2.4.5 Dielectric properties*

The dielectric properties of raw and char samples were measured at 2.45 GHz using a vector network analyzer from Keysight (model N5231A PNA-L) at room temperature. The sample powder was first crushed, loaded and then pressed in a 7-mm diameter coaxial airline from HP (model: 85051-60010). The complex permittivity of a dielectric material $\varepsilon$ can be given in equation 5 as:

$$\varepsilon\,(\omega) = \varepsilon'(\omega) - i\varepsilon''(\omega) \quad (5)$$

$$\tan\delta = \frac{\varepsilon''}{\varepsilon'} \quad (6)$$

The real component $\varepsilon'$ represents the storage ability of a material to store electrical energy of microwave while the imaginary component ε" represents the ability to lose this energy. The loss tangent ($\tan\delta$) which is given in equation 6 represent the efficiency of converting this electric energy into heat energy.

### *2.4.6 Electron spin resonance*

ESR spectra were collected at room temperature on a Magnettech MS-5000 spectrometer (Freiberg Instruments, Germany). Samples were placed inside a quartz capillary tube with a 0.75 mm wall thickness and a 5 mm outer diameter. The experiments were conducted with a microwave power (10 mW), a modulation width (0.2 mT), a magnetic field modulation (100 kHz) and a sweep width and time of 6200 G and 1 min, respectively. A solid standard sample of known weight of $CuSO_4 \cdot 5H_2O$ was used for calculating the number of spins in the sample signals. The spin concentration ($N_{s.spin}$) of a sample (directly proportional to the absorption area under the ESR curve) was calculated by comparing the double integrated areas of the sample ($A_{sample}$) signals, and standard ($A_{CuSO_4 \cdot 5H_2O}$) signals, related to the corresponding Q-factors of the sample and standard as shown in equation 7:

$$N_{s.spin} = \frac{N_A \cdot n_{CuSO_4 \cdot 5H_2O} \cdot A_{sample} \cdot Q_{CuSO_4 \cdot 5H_2O}}{A_{CuSO_4 \cdot 5H_2O} \cdot Q_{sample}} \qquad (7)$$

The spin sample concentration $C_{s.spin}$ [32] (equation 8) is given as the ratio between the number of spins and the weight of sample ($W_s$):

$$c_{s.spin} = \frac{N_{s.spin}}{W_s} \qquad (8)$$

The ESR g-factor is calculated from equation 9 [33] as:

$$g = \frac{H_1 \cdot \nu \cdot g_1}{H \cdot \nu_1} \qquad (9)$$

where $g_1$ is a constant factor (2.0028) of the strong pitch standard, H and $\boldsymbol{\nu}$ are positions and microwave frequencies of char samples, and $H_1$ and $\boldsymbol{\nu}_1$ are positions and microwave frequencies of the strong pitch standard. MatLab toolbox EasySpin 2.5 software was used in ESR-spectra fitting.

## 3 Results and discussion

### *3.1- Coal Pyrolysis*

#### *3.1.1- Product yields*

Figure 2a shows the distribution of gas, tar and char yields obtained from coal, biomass, and coal/biomass pyrolysis at 550 °C. In general, greater gas yields were observed under microwave pyrolysis for all tested samples, which could indicate increased secondary reactions under microwave heating compared to thermal heating. Microwaves produce localized hot spots within the material, which exhibit extreme temperatures and likely promote secondary cracking reactions yielding greater non-condensable gases. With addition of biomass to coal, gas yield decreased under both microwave and thermal pyrolysis methods, by 7.6 % and 11.3 %, respectively relative to pure coal samples. Greater gas yields were observed from biomass pyrolyis under both methods compared to that obtained from coal or coal/biomass, possibly due to the high volatile and oxygen content of biomass. Tar yield increased upon addition of biomass to coal regardless of the applied heating method. The tar yield increased from 6.0 wt.% (C-MW) to 19.5 wt.% (CB-MW), which is a factor of 3.26 under microwave pyrolysis, while it only increased from 15.0 wt.% (C-Conv) to 26.3 wt.% (CB-Conv), which is a factor of 1.75 under thermal pyrolysis. This result is possibly due to different free radical condensation and repolymerization reaction pathways under microwave and conventional thermal methods [34]. Pure biomass shows the greatest tar yield of all feedstocks. These results agree with the greater volatile matter of the parent biomass compared to coal. Overall, tar yields are lower under microwave pyrolysis for all samples, which is consistant with the greater gas yield obtained under microwave pyrolysis. Microwave tar yields for coal and coal/biomass samples are lower compared to thermal tars of these samples, possibly due to microwave selective excitation of polar groups facilitating decomposition to produce a higher gas yields compared to thermal pyrolysis [3a]. During biomass pyrolysis, similar gas, tar and char yields were observed regardless of the pyrolysis method used, possibly due to its low volatilization temperature compared to coal. Slightly lower char yields were observed under microwave coal and coal/biomass samples compared to thermal ones. This suggests an efficient interaction between microwave energy and coal especially in the presence of biomass, where the char yield decreased 6.8 % in the absence of biomass and 12.9 % in the presence of biomass when compared to thermal chars. In general, lower char yields were observed for pure biomass, followed by coal-biomass mixture, and then coal which had the highest char yield. These results agreed with the increasing fixed carbon and ash content of the studied samples shown in Table 1. As we go from biomass to coal samples, char yields are approximately equal to the sum of fixed carbon and ash of the parent feedstock.

During the thermal decomposition of coal or biomass, free radicals are formed [34]. These free radicals can either recombine via condensation or polymerization reactions into a stable polyaromatic coke or can abstract a proton and leave the reaction zone in the gas phase. These radical recombination mechanisms could be influenced by the applied heating mechanism whether it is through dielectric loss heating or conventional thermal heating. The high gas-to-tar yield ratio observed under microwave compared to thermal pyrolysis could suggest that. Under thermal pyrolysis high amounts of carbon were trapped into heavy tars and coke while under microwave the recombination rate of these radicals decreased leading to more gas formation. Selective decomposition of polar or microwave active tars, which have high dielectric properties, into gases could be enhanced under microwave pyrolysis [35].

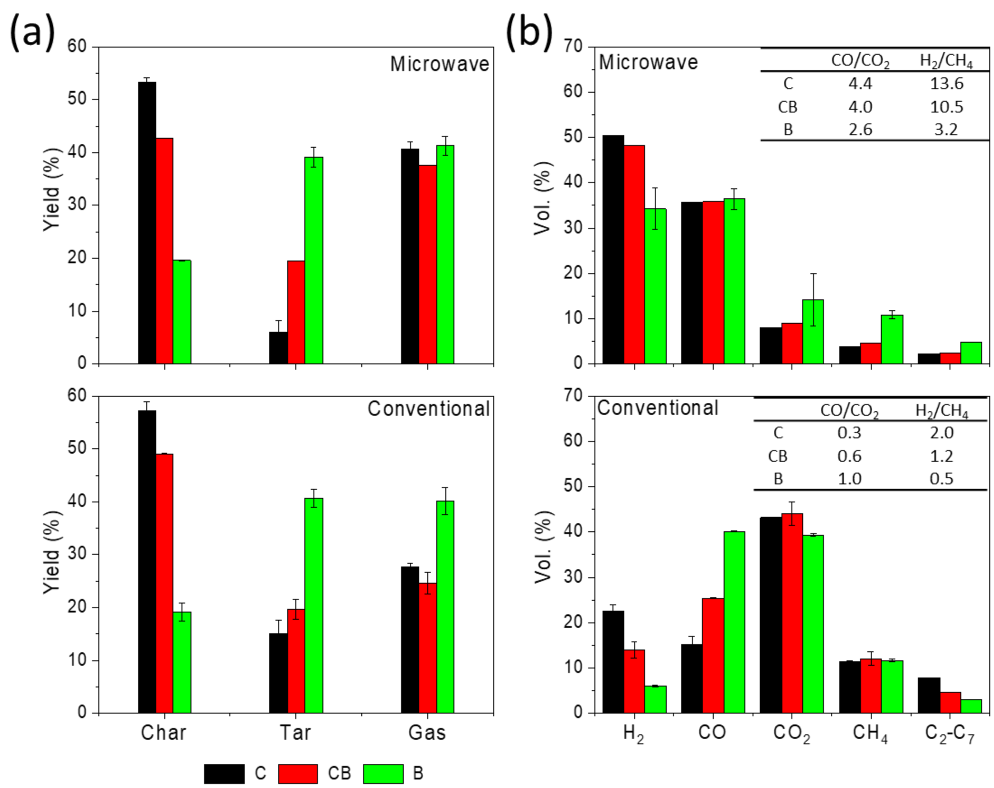


Figure 2. (a) yields of char, tar, and gas, and (b) total gas composition obtained during coal (C), coal/biomass (CB) and biomass (B) pyrolysis at 550 °C using microwave and thermal methods.

*3.1.2- Gas composition*

Figure 2b reveals the light gas composition ($H_2$, CO, $CO_2$, and $CH_4$) and light hydrocarbon species, from $C_2$ to $C_7$ produced during the pyrolysis reaction. For all samples, regardless of its composition, the selectivity towards syngas production was higher under microwave pyrolysis; the majority of gas composition was $H_2$ and CO. The $CO/CO_2$ ratios are much higher under microwave pyrolysis, ranging between 4.4 and 2.6, while they are between 0.3 and 1.0 under thermal pyrolysis. The high selectivity of CO could possibly be due to microwave-induced self-gasification reactions between the structural fixed carbon present in coal or biomass structure and the generated $CO_2$ producing more CO via the reverse Boudouard reaction ($CO_2 + C = 2CO$) [3a, 36]. Another possibility could be due to microwave-enhanced dry reforming between methane and $CO_2$ produced during pyrolysis in the presence of microwave-induced hotspots [37]; especially since the observed $CH_4$ concentrations are relatively low under microwave. As the biomass percentage in the microwave-heated samples increased, the CO, $CO_2$, $CH_4$ and $C_2$-$C_7$ % increased, and the $CO/CO_2$ ratio decreased from 4.4 for coal, 4.0 for coal/biomass, and down to 2.6 for biomass This is possibly due to the high density of oxygen-containing functional groups present in the biomass structure, the low fixed carbon content, and the high carbon-reactivity compared to coal. Functional groups present in coal, biomass, and their mixture could be heated and decomposed selectively under microwave irradiation leading to a different gas selectivities. On the other hand, addition of biomass under thermal pyrolysis results in increasing the CO selectivity compared to pure coal. The role of heating mechanism, whether via microwave or conventional thermal routes, affects the product selectivities of these gas species during pyrolysis. For example, the microwave selectivity towards $H_2$ and CO (syngas) is higher than it is under conventional thermal method, which is more selective towards $CO_2$ , $CH_4$ and $C_2$ to $C_7$ light hydrocarbons. These results suggest that the microwave could efficiently convert tars into syngas and possibly polyaromatic carbon.

Similarly, the gas composition analysis in Figure 2b (table inserts) demonstrated that under microwave pyrolysis the hydrogen is always more selectively produced than methane with much higher $H_2/CH_4$ ratios, ranging from 13.6 to 3.2, compared to thermal chars, ranging from 2.0 to 0.5, for all studied samples regardless of their composition. Selective decomposition of methane under microwave irradiation into carbon and $H_2$ or methane dry reforming could result in a higher $H_2$ selectivity under microwave pyrolysis. Addition of biomass to coal results in a drastic decrease in $H_2/CH_4$ ratio under microwave, whereas a relatively slight change in the $H_2/CH_4$ ratio was observed under thermal pyrolysis, mainly due to the decrease in $H_2$ concentration while the $CH_4$ concentration is relatively constant. The presence of biomass in a pyrolysis sample decreased the produced hydrogen regardless of the pyrolysis method used possibly due to the higher tar yields observed for biomass-based samples. Thermal decomposition of methoxy or bridged ether groups is very likely to take place during thermal pyrolysis of biomass. During pyrolysis, free-radicals are formed [34], and depending on their stability, smaller radicals could recombine to form low molecular weight hydrocarbon molecules in the gas phase. Different heating mechanisms, reaction rates, free radical recombination rates, and even different formation rates of these free radicals could play a role in the resulting product distribution during pyrolysis. These results confirm that choosing the right heating mechanism could help in tuning the product selectivity during coal and biomass pyrolysis.

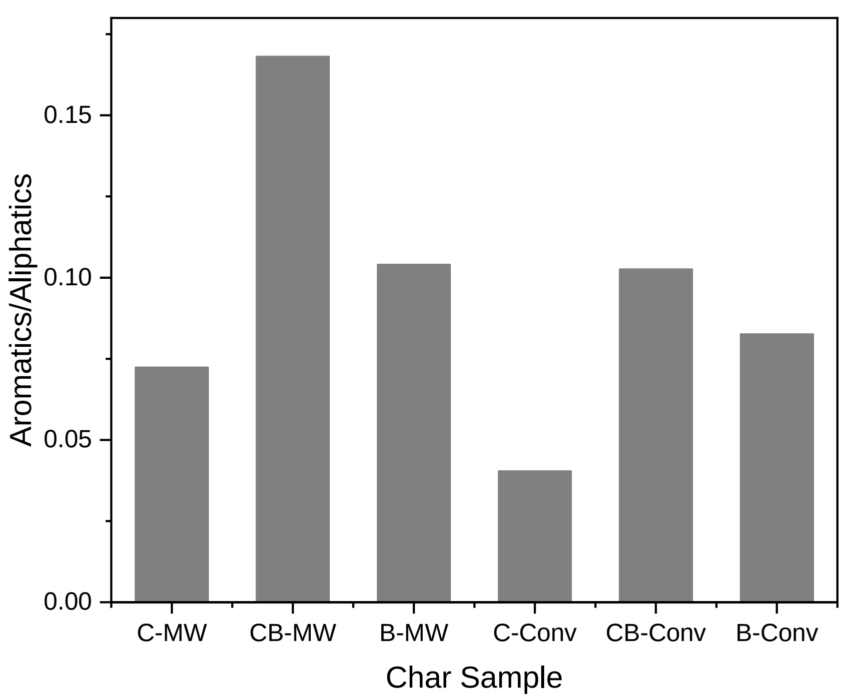

Figure 3. The molar ratio between aromatic ($C_6$-$C_7$) products and aliphatic ($C_2$-$C_4$) products obtained during coal (C), coal/biomass (CB) and biomass (B) pyrolysis at 550 ℃ using microwave and thermal methods.

The molar ratio between aromatic products, which is the total moles of benzene and toluene, to aliphatic hydrocarbons containing C2s (ethane, ethylene and acetylene), C3 (propylene), and C4 (1,3-butadiene) formed during pyrolysis are displayed in Figure 3. A higher aromatic-to-aliphatic fraction was observed under microwave and in the presence of biomass. The selective microwave heating could play a better role in coal depolymerization via targeting weak ether or alkyl linkages between aromatic compounds in coal or biomass samples compared to conventional thermal heating.

### *3.2- Char Properties*

#### *3.2.1- Surface area analysis*

The BET surface area, microporous surface and volume properties, and total pore volume are listed in Table 2. During pyrolysis pores develop as moisture and volatile organic compounds are released, leaving voids in the coal or biomass carbon matrix. The microwave-prepared chars had a higher surface area and pore volume than the conventional thermal chars, in dependent on the fuel source used whether it is pure coal or biomass or their blend. These results suggest that the applied heating mechanism could potentially alter the pore structure of these chars. Microwave energy could selectively gasify trapped carbon in presence of coal or biomass moisture which could lead to new pores in prepared chars during pyrolysis. Zhou et al[38] showed that during microwave drying of coal, moisture could rapidly change into superheated steam which affect the pore structure network of chars.  Further, coal or biomass particles experience greater volumetric heating rates under microwave treatment resulting in high pressures within the particle as volatiles are released. This rapid volatilization from the particle core also contributes to greater pore development under microwave heating compared to conventional thermal ones.

Biomass chars showed the highest surface properties among the studied samples with BET surface area of 138 $m^2/g$ and 71 $m^2/g$ generated under microwave and thermal pyrolysis, respectively. While coal chars had a lower surface area property with a BET of 96 $m^2/g$ and 61 $m^2/g$ generated under microwave and thermal pyrolysis, respectively. The high ash content in coal and differences in chemical structure between biomass and coal contribute to the lower surface area properties of coal chars regardless of the pyrolysis heating method. A recent study on the microwave pyrolysis on a biomass feedstock of coffee hulls shows similar results where a higher char porosity was achieved under microwave compared to conventional thermal method [39]. Lignocellulosic biomass, such as the pine wood used in this study, is composed of a matrix of cell walls. During pyrolysis volatile organic compounds leave the matrix, but the lignin-rich cell walls are not easily devolatilized and remain intact after thermal processing, leaving a porous matrix in the pyrolysis char. Coal, on the other hand, decomposed for millions of years and the plant cell wall structure is no longer intact. The regeneration of activated carbon was studied by Ania et al where the microwave regeneration relatively preserved its microporous and mesoporous structure, whereas conventional thermal regeneration, especially at elevated temperatures, results in a partial structure collapse [40]. Moisture removal could create new stable pores or even some pore enlargement via structure crosslinking[38] during microwave pyrolysis . In general, addition of biomass to coal enhanced the surface properties of generated char and could make it more reactive.

Table 2. Surface properties of collected chars.

| Heating Mode | Feedstock | $S_{BET}$ ($m^2/g$)^ | $S_{micro}$ ($m^2/g$)^^ | $V_{micro}$ ($cm^3/g$)^^ | $V_{total}$ ($cm^3/g$)^^^ |
|---|---|---|---|---|---|
| Microwave | C | 96 | 71 | 0.033 | 0.078 |
| | CB | 122 | 85 | 0.039 | 0.100 |
| | B | 138 | 110 | 0.051 | 0.081 |
| Thermal | C | 61 | 45 | 0.021 | 0.062 |
| | CB | 64 | 48 | 0.022 | 0.057 |
| | B | 71 | 13 | 0.005 | 0.079 |

^ BET method was used up to $P/P^o = 0.2$.
^^ *t*-plot method was used.
^^^ $V_{total}$ @ $P/P^o = 0.985$.

### *3.2.2- Electron microscopy*

Figure 4 shows the SEM images for fresh and generated chars of pure coal and biomass samples. Microwave coal and biomass chars shows a relatively similar morphologies with microsphere structures on the char surfaces and with high surface porosity. These microspheres are more uniformly distributed with a narrow average size distribution in case of microwave biomass char B-MW sample compared to C-MW sample. The corresponding conventional thermal chars showed big particle aggregates for coal and fiber-like aggregates for biomass chars. Both are with less surface porosity compared to corresponding microwave chars agreeing with the observed surface area results in section 3.1. The heating mechanism applied plays an important role in shaping the surface morphologies of the prepared chars.

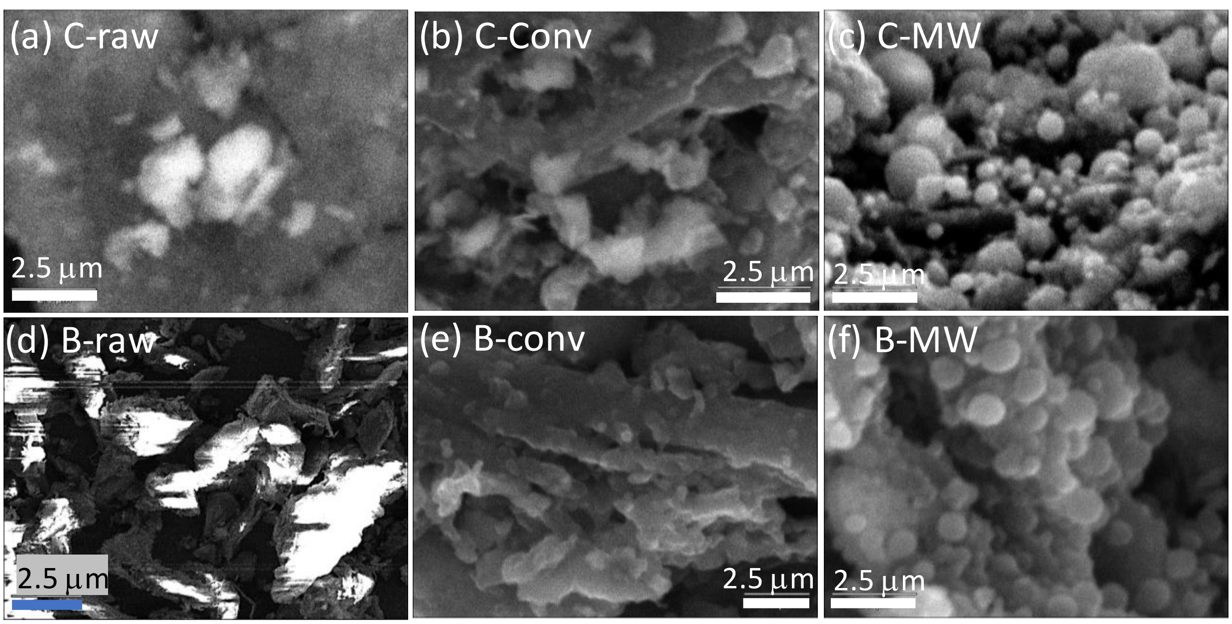


Figure 4. SEM images of raw and pyrolyzed chars under thermal and microwave methods for coal (a, b, and c) and biomass (d, e, and f), respectively.

Surface functionality of coal and biomass with organic polar groups as carboxyl, carbonyl, aldehyde, or hydroxyl groups could represent the active microwave sites that could get heated via dipole loss mechanism[41] under microwave irradiation. This could lead to the formation of hot spots leading to microsphere formation and some internal morphological changes under microwave heating[42].

The specific morphologies obtained from coal and biomass by either thermal or microwave pyrolysis could provide insight on the surface chemistry which could help guide utilization of chars for conversion to value added products. For example, the char morphology and high surface area generated by microwave heating would make them suitable as precursors for activated carbon or catalyst application. By comparison, those generated under thermal heating would be less desirable for these applications.

### *3.2.3- X-ray crystallinity*

Figure 5 shows the diffraction patterns of all prepared chars. The diffractograms for biomass-derived char exhibit two broad peaks that could be emerged from some ordered carbon domains or carbonized structures within the biochar matrices. These broad diffraction bands between 20° and 30 ° and between 40° and 50 ° could be assigned to graphitic diffraction planes (002) and (100), respectively [41a]. These broad peaks were observed for biomass chars prepared by both microwave and thermal pyrolysis and are typical of amorphous and turbostratic carbonaceous phases. Coal chars also exhibit broad (002) and (100) carbon diffraction peaks indicating the presence of an amorphous carbon phase, albeit less intense than those of biomass chars. The carbon peaks are likely masked by the abundance of inorganic phases due to the high ash content of the parent coal. Upon heating coal, biomass, or their mixture, volatiles are released and aromatic molecules crosslink with the char resulting in carbon structural rearrangement. Depending on the pyrolysis conditions, the carbon stacking and ordered structure differ [43].

Carbon was found to be more ordered in biomass chars compared to coal chars due to the high ash content and the nature of chemical composition of coal compared to biomass. The oxygen-containing functional groups found in biomass could lead to selective heating under microwave. It is also obvious that the nature of carbon in microwave biochar is more developed than in conventional thermal biochar, where the carbon

(002) peak is more pronounced. Similar diffraction patterns were observed for microwave and thermal coal chars, where almost no carbon peaks could be observed. The addition of biomass to coal has increased the graphitic nature of the generated char under microwave while it remained the same under thermal pyrolysis; it can be observed from the evolution of broad peaks in the carbon diffraction regions. In general, the more the staking of the carbon rings in the prepared chars, the higher its graphitic nature and the more lossy it became under microwave irradiation [43b].

Coal- and coal/biomass-derived chars prepared by both microwave and conventional thermal heating exhibit intense peaks at 26.6 ° corresponding to $SiO_2$. Coal chars have a high ash content, which is composed of 45.3% Si according to coal ash analysis (Table 1). This peak is also observed for biomass chars, although it is less intense due to the much lower ash content of the parent biomass. In addition to the observed sharp crystalline peaks of $SiO_2$, CaS crystalline peaks were only observed under microwave pyrolysis of coal and coal-biomass chars and not observed under thermal pyrolysis. The localized hot spots formed under the dielectric heating of microwave could enhance the carbothermic reduction of $CaSO_4$ in presence of coal carbon to produce CaS and $CO_2$ [44].

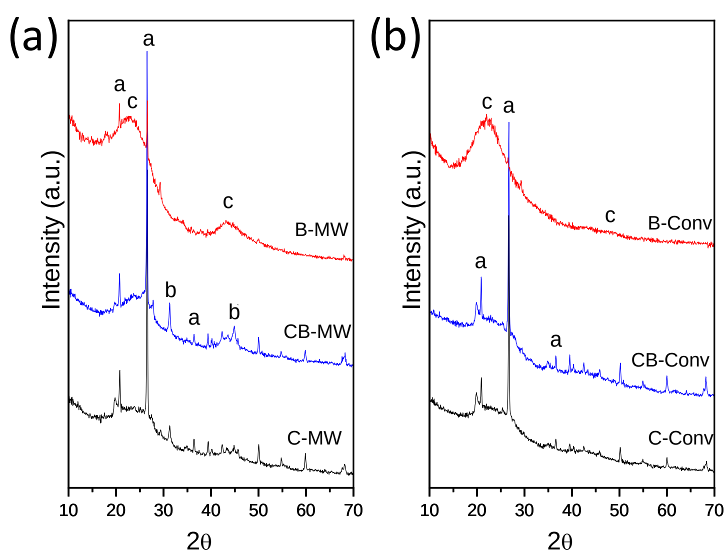


Figure 5. Diffraction patterns for coal, coal-biomass, and biomass chars prepared under (a) microwave and (b) thermal pyrolysis methods. (a: $SiO_2$, b: CaS, c: carbon).

*3.2.4- Raman analysis*

The graphitic nature of carbon in the prepared chars were examined using Raman spectroscopy in the first order band between 1000 $cm^{-1}$ and 1800 $cm^{-1}$region [45]. Figure 6 shows the Raman spectra of these chars, where they were best fitted into four bands each. Three were Lorentzian fitted: G, $D_1$, and $D_4$ at about 1580 $cm^{-1}$, 1350 $cm^{-1}$, and 1200 $cm^{-1}$, respectively and one was Gaussian fitted; $D_3$ at about 1500 $cm^{-1}$. Polycrystalline carbon of highly ordered graphite sheets has a G-band at around 1580 $cm^{-1}$ and a defect $D_1$-band at 1350 $cm^{-1}$ . The G-band is characterized with a sharp high intensity signal that is due to the $E_{2g}$ lattice vibrations and the $D_1$-band is due to lattice defects with $A_{1g}$ symmetry [46] and is characterized with a weak broad signal. Additional D bands could be observed in the Raman spectrum depending on the degree of carbon ordering in the char. Raman peak deconvolution can account for degree of carbon crosslinking in char, how big is the domains of aromatic rings in char, and extent of substitution [47]. The $D_3$ band is usually between G and $D_1$ bands at about 1500 $cm^{-1}$. $D_3$ band is assigned to amorphous mixed carbon [48] thus it could be used to measure the degree of thermal stability under oxygen [45].

The intensity of G-band at 1580 $cm^{-1}$ increased with respect to $D_1$-band intensity at 1350 $cm^{-1}$ as we went from coal to biomass char generated under microwave pyrolysis. The band area ratios between $I_G/I_{All}$ and $I_{D1}/I_G$ were calculated and listed in Table 3 where $I_{All}$ accounts for the total area integrated under the Raman spectrum peaks. For pure coal char, the $I_G/I_{All}$ did not change significantly between microwave nor conventional thermal pyrolysis which agrees with the observed similarity in their corresponding XRD patterns shown in Figure 5. Addition of biomass to coal has increased the intensity of G-band, only in the CB-MW char sample while it remained the same for thermal char (CB-Conv) compared to pure coal char, indicating that the carbon ordering in microwave char has increased in the presence of biomass. For pure biomass char, the $I_G/I_{All}$ ratio increased under microwave compared to under thermal. In general, the most carbon-ordered chars were observed for microwave chars: CB-MW and B-MW, which indicate that the presence of biomass during microwave coal pyrolysis assisted in an efficient microwave absorption. The addition of biomass increased the graphitic nature of microwave generated chars compared to its addition during thermal pyrolysis.

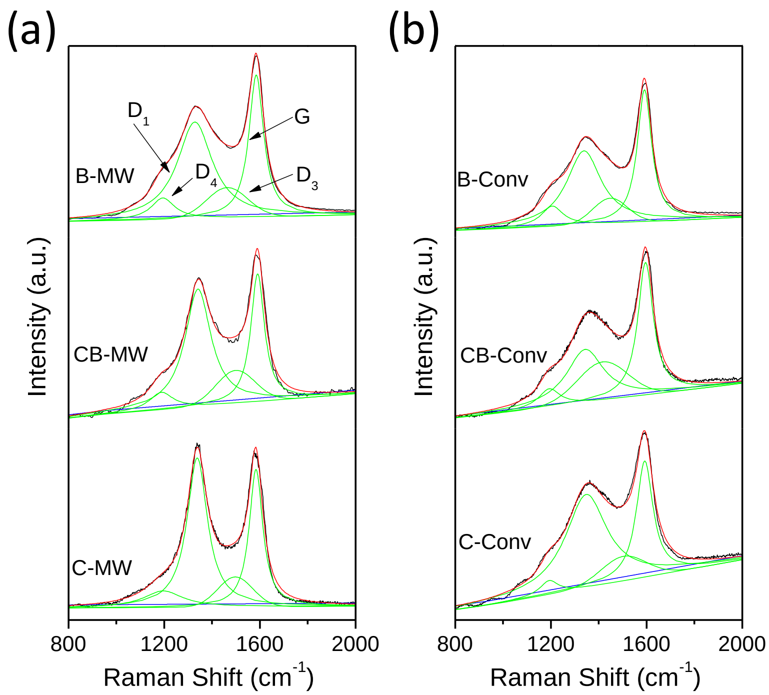


Figure 6. Raman spectra for chars prepared under (a) microwave and (b) thermal methods.

Table 3. Band area ratios and microcrystalline carbon sizes calculated for microwave and thermal chars.

| Fuel composition | Char Sample | Band area ratio | | $L_a$[#] (nm) |
|---|---|---|---|---|
| | | $I_G/I_{All}$ | $I_{D1}/I_G$ | |
| Coal | C-MW | 0.29 | 2.00 | 2.20 |
| | C-Conv | 0.30 | 2.00 | 2.20 |
| Coal-Biomass | CB-MW | 0.36 | 0.96 | 4.60 |
| | CB-Conv | 0.29 | 1.75 | 2.51 |
| Biomass | B-MW | 0.35 | 1.34 | 3.29 |
| | B-Conv | 0.31 | 1.60 | 2.74 |

[#] $L_a$ was calculated from equation 4.

Also, in microwave chars the Raman peaks are narrower compared to conventional char peaks. D-band broadening is a result of heteroatoms and the wide range in the size of ring systems. Pyrolysis intensification by microwaves destroyed side chains and oxygen-containing functional groups leading to a more condensed aromatic ring system in the char, especially in the case of coal. The D-band for biomass char prepared by microwave is broader than that of coal char, indicating the presence of oxygen functional groups and side chains in the char structure. Biomass char may also have a wider range of ring system sizes compared to coal char.

The planer size ($L_a$) of microcrystalline carbon in chars were calculated [31] and are shown in Table 3. $L_a$ is a measure of the long-range order in the carbon lattice structure. Calculated $L_a$ ranged from about 2.2 nm to 4.6 nm for the studied chars. Similar $L_a$ were observed for coal chars at 2.2 nm regardless of the applied pyrolysis method. With addition of biomass to coal, $L_a$ increases to 4.6 nm, and 2.5 nm under microwave and thermal pyrolysis, respectively. Similarly, biochar generated under microwave shows a higher $L_a$ compared to that under thermal pyrolysis, likely due to the selective heating nature under microwave compared to under a conventional thermal method. Xu el al. [49] have correlated the carbon structure and its graphitic nature of carbon in chars using Raman and dielectric properties of chars.

*3.2.5- Dielectric properties*

Dielectric property measurements of the produced chars further indicate the carbon ordering of chars after pyrolysis, especially those prepared under microwave heating (Table 4). Chars from thermal pyrolysis of coal and biomass have dielectric properties with values close to those of raw coal and raw biomass. Chars prepared under microwave heating have a greater dielectric constant and dielectric loss factor than those prepared under conventional thermal heating. The greater permittivity values could be a result of increased mobility of pi-electrons between char interlayers, indicating enhanced ordering of char structure due to microwave heating. During thermal processing, volatiles are released as the feedstock is converted to carbonaceous char. Under conventional thermal heating, high molecular weight oxygenates remain in the char, but under microwave heating the polar functional groups are selectively heated and the high molecular weight compounds volatilize. While the bulk material temperature is fixed at 550 °C under both modes of heating, microwave heating creates extreme local hot spots within the material which promotes greater bond cleavage than conventional thermal heating.

The loss tangent (*tan* $\delta = \varepsilon''/\varepsilon'$) is a useful parameter for evaluating the dielectric heating susceptibility of a material under an electric field. Loss tangent is found to be greater for chars prepared under microwave heating; thus, these chars are expected to have greater ability to generate heat under a microwave field compared to those prepared under conventional thermal heating. As described above, this is attributed to the greater mobility of pi-electrons within the ordered aromatic char structure. This is especially the case for coal chars as they are more aromatic in nature than biomass chars. Further, biomass char contains more oxygenated compounds than coal, some of which have oxygen molecules embedded in a ring structure, such as those species derived from cellulose, hemicellulose or lignin [50]. These oxygenates remain in the biomass char structure, resulting in less aromaticity compared to coal chars. This result is consistent with the Raman spectroscopic data, in which biomass chars possess a broader defect band due to oxygen impurities. Differences in biomass and coal char dielectric properties could also be attributed to the high ash content in coal-derived char. Inorganic phases in the coal char may be polarizable by ionic conduction, resulting in greater permittivity values compared to biomass char. Additionally, an enhancement is observed when coal and biomass are pyrolyzed together under microwave irradiation. Microwave pyrolysis generates a high yield of H and –OH radicals from biomass decomposition, which act as H donors in the presence of coal free radicals. This promotes condensation reactions within the char structure, forming polycyclic aromatic systems in the char with delocalized pi electrons and resulting in an increased loss tangent. This result is consistent with the high $L_a$ value of microwave-generated chars from the coal and biomass mixture as calculated from Raman spectroscopic data.

Table 4: Char dielectric properties at 2.45 GHz produced by pyrolysis of coal, coal/biomass, and biomass under microwave and conventional thermal heating at 550 °C for 2 hours.

| | ε' | | | ε"/ε' | | |
|---|---|---|---|---|---|---|
| | Raw | MW | Conv | Raw | MW | Conv |
| Coal | 2.27 | 6.38 | 2.31 | 0.21 | 0.51 | 0.19 |
| Coal-Biomass | | 12.38 | 2.26 | | 0.84 | 0.18 |
| Biomass | 1.63 | 3.94 | 1.43 | 0.16 | 0.53 | 0.11 |

*3.1.6- Electron spin resonance spectroscopy*

ESR study on char samples could help in understanding the char reactivity where higher radical concentration indicates that the char has a higher reactivity whereas low radical concentration is always associated with stable radicals. In addition, ESR data can shed some light on the carbon structure and the polyaromatic density in generated chars. The spin concentrations and g values of original fuels and their chars are shown in Figure 7. The radical concentrations ranged from between 34 x $10^{16}$ spins $g^{-1}$ to 105 x $10^{17}$ spins $g^{-1}$. The microwave-pyrolyzed coal showed a significantly higher concentration of radicals compared to the biomass char under similar operating conditions, probably due to the formation of small polyaromatic hydrocarbon (PAH) radicals in the coal microwave pyrolysis. The addition of biomass to coal microwave pyrolysis decreased the radical concentration drastically possibly due to synergistic effects between coal and biomass. The presence of biochar heats coal sample efficiently during microwave pyrolysis. Interestingly, the radical concentrations in the coal char matrix and mixed coal/biomass char from thermal pyrolysis were similar, possibly due to the similar polyaromatic origin of chars.

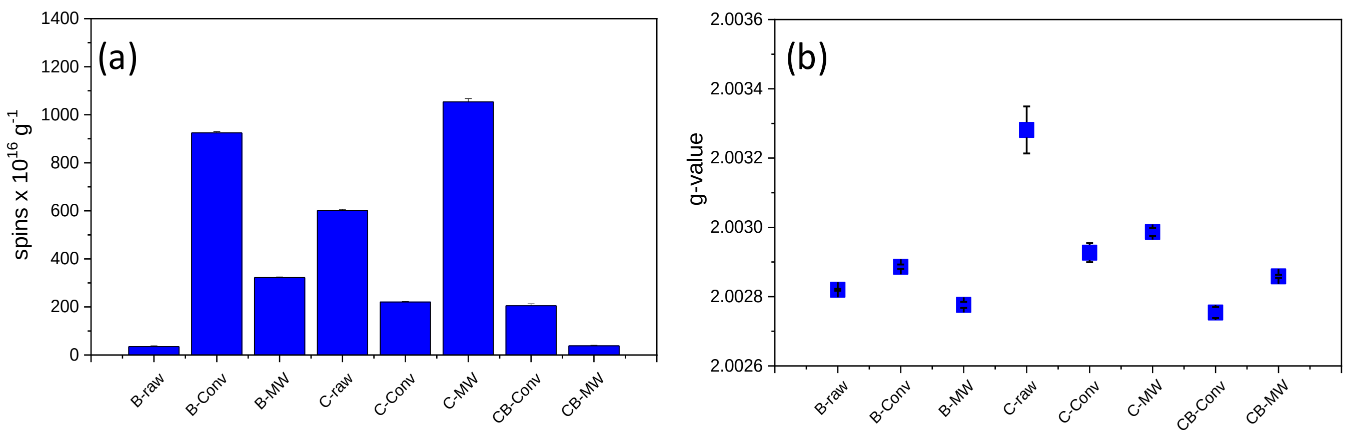


Figure 7. (a) radical concentration (spins x $10^{16}$ $g^{-1}$) and (b) g-value of original fuels and the corresponding chars.

The present results emphasize the importance of heating rate on the synergistic effect on the coal conversion. Hydrogen and OH radicals formed during biomass pyrolysis can promote cracking of the aromatic rings of coal under fast heating rates[8b, 51]. Catalytic effects of alkali metals in biomass can promote synergistic effects between biomass and coal[52]. Hemicellulose might also provide a strong synergistic effect on the coal conversion during co-pyrolysis[53]. The holocelluloses are mainly responsible for the volatile release during pyrolysis, and further production of hydrogen by secondary reactions. Previous results showed that the synergistic effect of legume straw with higher holocellulose and ash content was more significant than that in the presence of pinewood sawdust with the similar holocellulose and lower alkali contents during co-pyrolysis with coal in a free-fall reactor[5d]. In the present study, the wood sample was low alkali-containing. Thus, only high content of holocellulose in the wood sample provided a strong synergistic effect on the radical formation. Lignin affects the polymerization reactions, resulting in the formation of stable phenoxy and other reactive radicals [24b, 54]. The short-lived radicals are effective and active intermediates to depolymerize coal by cleaving methylene bridges[5b]. The coal structure is disturbed during microwave pyrolysis, leading to a strong fragmentation of coal into hydrogen deficient active sites. Biomass has a higher H/C ratio than coal, and the availability of hydrogen around the coal particles increases during microwave co-pyrolysis. The free radicals from biomass react with the polymerizing structure of coal char and enhance its decomposition during pyrolysis. The volatiles released from biomass are rich in hydrogen that reacts with coal radicals, and thus, prevent the recombination and cross-linking reactions, resulting in the low char yield at fast heating rates of microwave pyrolysis. Hydrogen released in biomass pyrolysis and also hydrogen abstracted from the aliphatic species prevent cross-linking reactions and produced the high yields of tars before the cross-linking occurred [55]. The current results showed that the co-pyrolysis of low-ranking coal and biomass increased the formation of tars and subsequently decreased the char yields in microwave pyrolysis. The tar yields in microwave pyrolysis of both coal and biomass/coal blends were lower than the tar yields formed during thermal pyrolysis. The tar yield reaches a maximum value at intermediate temperatures (300-500 °C) and decreases at higher temperatures (800-1000 °C) due to thermal cracking of heavy compounds in microwave pyrolysis[56].

The radical concentration remained unaffected by the biomass addition in thermal coal pyrolysis. The extended residence time of intraparticle volatiles in thermal pyrolysis allows for increased extra particle secondary reactions, leading to the formation of stable large PAH radicals[57]. Thus, the synergistic effect with the addition of biomass to coal pyrolysis is less dominating at slow heating rate. The yields of $H_2$ and CO in microwave pyrolysis increase significantly due to the reforming of $CH_4$ and $CO_2$ compared to the thermal pyrolysis[8a].

The low radical concentration can indicate that the char contains conductive carbon species or maybe some paramagnetic metals such as Mg or Fe [58]. A correlation between the radical appearance and the tar formation mechanism is still debatable in literature [54]. Coal-biomass will repolymerize faster and form larger polyaromatic clusters than coal which form smaller PAH, and the repolymerization and cross-linking reaction time is significantly longer.

Table 5: g-values of free radicals present in raw coal, biomass and their chars[26b].

| **g-factor** | **Description** | **Ref.** |
|---|---|---|
| | **Carbon-based radicals** | |
| 2.0025 – 2.0026 | Aliphatic pi type radicals on hydrocarbons | 24b |
| 2.0026 – 2.0028 | 1-5 rings aromatic hydrocarbons | 24b |
| 2.0028 | Graphitic carbon, unsubstituted aliphatic radical | 55a, 59 |
| 2.0029 | Complex aromatic hydrocarbons (corocene, benzoperylene) | 24b |
| 2.003 – 2.004 | Carbon center with an oxygen atom | 55b |
| 2.0030 – 2.0035 | Azoaromatics | 32 |
| 2.0035 – 2.0042 | Azo compounds | 32 |
| | **Oxygen-based radicals** | |
| 2.0038 – 2.0047 | Pi type radicals (quinones, 1-3 rings) | 24b |
| 2.0035 – 2.0040 | Ethers (mono-, di-, and trimethoxybenzenes) | 24b |
| 2.0040 – 2.0060 | ketyl anions, semiquinone, semidioone | 32 |
| | **Nitrogen-based radicals** | |
| 2.0031 | Nitrogen containing radicals | 24b |
| 2.0045 – 2.0055 | Nitro compounds | 32 |
| 2.0055 – 2.0065 | Nitroxyls | 32 |

The radical concentration in coal char from the thermal pyrolysis is low compared to biomass. This is due to the greater concentration of alkali metals (potassium) in coal compared to biomass that is known to reduce the formation of radicals during slow pyrolysis [60]. The presence of potassium can weaken the C-C bonds in aromatic rings and therefore, could facilitate its breakage during pyrolysis which leads to the formation of aliphatic radicals. These radicals could polymerize into stable polyaromatic hydrocarbons (PAH) at an early stage of the coal pyrolysis[61]. Moreover, the high content of silicon in coal could lead to the formation of silicates, which might trap the radicals in the glassy coal char matrix, and thus, the radical concentration in coal is lower than in thermal biomass pyrolysis [62]. Interestingly, the radical concentrations in the coal char and mixed coal and biomass char from the thermal pyrolysis were similar. This indicates that the biomass composition has no influence on the radical formation in the co-pyrolysis of coal and biomass. This is probably due to the more dominating catalytic effect of alkali and presence of a greater amount of silicon in the coal than in biomass.  Greater radical concentrations in the woodchip chars and mixed coal/biomass chars from the decay stage of thermal pyrolysis compared to the woodchip chars and mixed coal/biomass chars from microwave pyrolysis may be related to the more efficient catalytic effects of potassium on the bond-breaking and radical re-attachments, as the previous results have shown[62a, 63]. The greater radical concentration was observed in the coal char from microwave pyrolysis compared to that from thermal pyrolysis. The presence of pyrite in coal enhances the formation of free radicals during pyrolysis. At temperatures 500-550 °C close to 60 % sulfur in the coal has been released during thermal pyrolysis, and the remaining sulfur was bonded as organic sulfur to the coal char matrix, leading to the less influence on the radical formation [64]. However, the microwave-assisted pyrolysis of coals is based on the fact that coal releases pyrite more rapidly than during thermal pyrolysis due to the enhanced magnetic susceptibility of pyrite. The formation of radicals might be also enhanced by the presence of calcite in addition to pyrite that participates in the cracking reactions of oxygen functional groups and aromatics during microwave-assisted pyrolysis of coal [65].

Since the ESR results for coal char microwaved at elevated temperature (900 °C) has no ESR signal and a very low radical concentration (data not shown here), addition of biomass to coal at 550 °C under microwave could result in increasing localized temperature zones during microwave irradiation and assist in heating up and converting coal into char with low ESR signal (lowest observed at 550 °C pyrolysis). In other words, the presence of biomass, which can convert easier into conductive biochar under microwave irradiation, absorb and couple more efficiently with microwave energy (CB-MW char sample showed the highest dielectric properties) and assist during coal pyrolysis into almost complete coal char is beneficial. This trend was confirmed with coal char collected at 900 °C using microwave (no ESR signal detected) indicating a complete conversion into char.

Figure 7b shows the calculated *g*-values using equation 9. The *g*-values of all samples are between 2.0027 and 2.0032 indicating the absence of sulfur-containing radicals which has a higher *g*-values between 2.0080 and 2.0081. The overlapping between nitrogen-containing and oxygen-containing radicals with a *g*-value of 2.0031 [66] could indicate the presence of nitrogen radicals in raw coal since it shows a *g*-value greater than 2.0030. Figure 7b also showed that the PAH-based defect structures which usually has a *g*-value less than 2.0040 were not present in all measured samples [67]. This indicates that the biomass, coal, and mixed chars mainly contained radicals which are stable hydroxylated PAH-based structures. The chars prepared under microwave and thermal pyrolysis conditions contained spectra with *g*-values between 2.0027 and 2.0029, suggesting the presence of carbon-centered radicals which is between *g* values of 2.0025 and 2.0030 [24b, 59]. Free radicals with higher *g*-values, as listed in Table 5, or even oxygen-centered radicals with *g* values between 2.0038 and 2.0047 [24b] were not observed possibly due to thermal decomposition of oxygen-containing groups during pyrolysis via decarboxylation, dehydration, or ether breaking reactions. Radicals in the biomass and coal chars from both thermal and microwave pyrolysis could have polyaromatic hydrocarbons (PAH) with 1 to 5 rings (*g* values between 2.0026 and 2.0028) with low concentration of carbon-centered radicals that contains oxygen [68]. The *g*-value of raw coal decreased after pyrolysis and upon addition of biomass to coal where the *g*-value of coal char is higher than coal-biomass char.

## 4. Conclusion

This work has demonstrated a novel method for the reduction of toxic free radicals using microwave co-pyrolysis of coal and biomass. Importantly, it has been shown for the first time that microwave co-pyrolysis of biomass and coal leads to significantly higher syngas yields with the minimal production of liquid and solid products compared to thermal pyrolysis. Microwaves could heat the biomass in the blend sample and strip out its polar groups selectively and convert it into an active microwave absorber that can decompose coal efficiently and promote faster devolatilization rates during the co-pyrolysis process. A synergistic effect was observed upon biomass addition during microwave coal pyrolysis. Electron spin resonance spectroscopy revealed that the microwave coal/ biomass char is the most stable char with the lowest free radical concentration. The microwave pyrolysis of both coal and co-pyrolyzed coal and biomass significantly improved the char properties by making the carbonaceous matrix more graphitic and thus, less reactive. Therefore, the work described here shows a great promise for using microwave co-pyrolysis of coal and biomass as a renewable reductant in metallurgical industries.

## 7 References

1. Annual Energy Outlook 2018. U.S. Energy Information Administration: 2018.

2. (a) Savolainen, K., Co-firing of biomass in coal-fired utility boilers. *Applied Energy* **2003,** *74* (3), 369-381; (b) Pérez-Jeldres, R.; Cornejo, P.; Flores, M.; Gordon, A.; García, X., A modeling approach to co-firing biomass/coal blends in pulverized coal utility boilers: Synergistic effects and emissions profiles. *Energy* **2017,** *120*, 663-674.

3. (a) Abdelsayed, V.; Shekhawat, D.; Smith, M. W.; Link, D.; Stiegman, A. E., Microwave-assisted pyrolysis of Mississippi coal: A comparative study with conventional pyrolysis. *Fuel* **2018,** *217*, 656-667; (b) Lin, X.; Luo, M.; Li, S.; Yang, Y.; Chen, X.; Tian, B.; Wang, Y., The evolutionary route of coal matrix during integrated cascade pyrolysis of a typical low-rank coal. *Applied Energy* **2017,** *199*, 335-346; (c) Cui, T.; Fan, W.; Dai, Z.; Guo, Q.; Yu, G.; Wang, F., Variation of the coal chemical structure and determination of the char molecular size at the early stage of rapid pyrolysis. *Applied Energy* **2016,** *179*, 650-659.

4. (a) Daniel, D. J.; Ellison, C. R.; Bursavich, J.; Benbow, M.; Favrot, C.; Blazier, M. A.; Marculescu, C.; Nokes, S. E.; Boldor, D., An evaluative comparison of lignocellulosic pyrolysis products derived from various parts of Populus deltoides trees and Panicum virgatum grass in an inductively heated reactor. *Energy Conversion and Management* **2018,** *171*, 710-720; (b) Henkel, C.; Muley, P. D.; Abdollahi, K. K.; Marculescu, C.; Boldor, D., Pyrolysis of energy cane bagasse and invasive Chinese tallow tree (Triadica sebifera L.) biomass in an inductively heated reactor. *Energy Conversion and Management* **2016,** *109*, 175-183; (c) Klinger, J. L.; Westover, T. L.; Emerson, R. M.; Williams, C. L.; Hernandez, S.; Monson, G. D.; Ryan, J. C., Effect of biomass type, heating rate, and sample size on microwave-enhanced fast pyrolysis product yields and qualities. *Applied Energy* **2018,** *228*, 535-545.

5. (a) Aboyade, A. O.; Görgens, J. F.; Carrier, M.; Meyer, E. L.; Knoetze, J. H., Thermogravimetric study of the pyrolysis characteristics and kinetics of coal blends with corn and sugarcane residues. *Fuel Processing Technology* **2013,** *106*, 310-320; (b) Quan, C.; Gao, N., Copyrolysis of Biomass and Coal: A Review of Effects of Copyrolysis Parameters, Product Properties, and Synergistic Mechanisms. *BioMed Research International* **2016,** *2016*, 11; (c) Wu, Z.; Li, Y.; Xu, D.; Meng, H., Co-pyrolysis of lignocellulosic biomass with low-quality coal: Optimal design and synergistic effect from gaseous products distribution.

*Fuel* **2019,** *236*, 43-54; (d) Wei, L.-g.; Zhang, L.; Xu, S.-p., Effects of feedstock on co-pyrolysis of biomass and coal in a free-fall reactor. *Journal of Fuel Chemistry and Technology* **2011,** *39* (10), 728-734.

6. (a) Vyas, A.; Chellappa, T.; Goldfarb, J. L., Porosity development and reactivity changes of coal–biomass blends during co-pyrolysis at various temperatures. *Journal of Analytical and Applied Pyrolysis* **2017,** *124*, 79-88; (b) Guan, Y.; Ma, Y.; Zhang, K.; Chen, H.; Xu, G.; Liu, W.; Yang, Y., Co-pyrolysis behaviors of energy grass and lignite. *Energy Conversion and Management* **2015,** *93*, 132-140.

7. Moghtaderi, B.; Meesri, C.; Wall, T. F., Pyrolytic characteristics of blended coal and woody biomass. *Fuel* **2004,** *83* (6), 745-750.

8. (a) An, Y.; Tahmasebi, A.; Yu, J., Mechanism of synergy effect during microwave co-pyrolysis of biomass and lignite. *Journal of Analytical and Applied Pyrolysis* **2017,** *128* (Supplement C), 75-82; (b) Wu, Z.; Wang, S.; Zhao, J.; Chen, L.; Meng, H., Synergistic effect on thermal behavior during co-pyrolysis of lignocellulosic biomass model components blend with bituminous coal. *Bioresource Technology* **2014,** *169* (Supplement C), 220-228.

9. (a) Krerkkaiwan, S.; Fushimi, C.; Tsutsumi, A.; Kuchonthara, P., Synergetic effect during co-pyrolysis/gasification of biomass and sub-bituminous coal. *Fuel Processing Technology* **2013,** *115*, 11-18; (b) Zhou, L.; Zhang, G.; Reinmöller, M.; Meyer, B., Effect of inherent mineral matter on the co-pyrolysis of highly reactive brown coal and wheat straw. *Fuel* **2019,** *239*, 1194-1203.

10. Vuthaluru, H. B., Thermal behaviour of coal/biomass blends during co-pyrolysis. *Fuel Processing Technology* **2004,** *85* (2), 141-155.

11. Lam, S. S.; Chase, H. A., A Review on Waste to Energy Processes Using Microwave Pyrolysis. *Energies* **2012,** *5* (10), 4209-4232.

12. N. Saifuddin, P. P. a. S. B. H., Microwave-Assisted Co-Pyrolysis of Bamboo Biomass with Plastic Waste for Hydrogen-Rich Syngas Production *American Journal of Applied Sciences* **2016,** *13* (5), 511-521.

13. (a) Zhao, X.; Guo, B.; Wang, W.; Chen, G.; Mao, Y.; Sun, J.; Song, Z., Experimental study on microwave pyrolysis of three Chinese lignite. *Journal of Analytical and Applied Pyrolysis* **2017,** *124*, 303-309; (b) Wu, C.; Budarin, V. L.; Gronnow, M. J.; De Bruyn, M.; Onwudili, J. A.; Clark, J. H.; Williams, P. T., Conventional and microwave-assisted pyrolysis of biomass under different heating rates. *Journal of Analytical and Applied Pyrolysis* **2014,** *107*, 276-283.

14. Zhang, Y.; Fan, L.; Liu, S.; Zhou, N.; Ding, K.; Peng, P.; Anderson, E.; Addy, M.; Cheng, Y.; Liu, Y.; Li, B.; Snyder, J.; Chen, P.; Ruan, R., Microwave-assisted co-pyrolysis of brown coal and corn stover for oil production. *Bioresource Technology* **2018,** *259*, 461-464.

15. Shi, K. Q.; Wu, T.; Zhao, H. T.; Lester, E.; Wang, Y. D., Microwave Induced Co-Processing of Biomass/Coal Blends. *Applied Mechanics and Materials* **2013,** *319*, 227-232.

16. Zhang, Y.; Zhao, W.; Li, B.; Xie, G., Microwave-Assisted Pyrolysis of Biomass for Bio-Oil Production: A Review of the Operation Parameters. *Journal of Energy Resources Technology* **2018,** *140* (4), 040802-040802-6.

17. Uzoejinwa, B. B.; He, X.; Wang, S.; Abomohra, A. E.-F.; Hu, Y.; He, Z.; Wang, Q., Co-pyrolysis of macroalgae and lignocellulosic biomass. *Journal of Thermal Analysis and Calorimetry* **2018**.

18. Tan, X.-f.; Liu, S.-b.; Liu, Y.-g.; Gu, Y.-l.; Zeng, G.-m.; Hu, X.-j.; Wang, X.; Liu, S.-h.; Jiang, L.-h., Biochar as potential sustainable precursors for activated carbon production: Multiple applications in environmental protection and energy storage. *Bioresource Technology* **2017,** *227*, 359-372.

19. Shen, Y.; Zhao, P.; Shao, Q.; Ma, D.; Takahashi, F.; Yoshikawa, K., In-situ catalytic conversion of tar using rice husk char-supported nickel-iron catalysts for biomass pyrolysis/gasification. *Applied Catalysis B: Environmental* **2014,** *152-153*, 140-151.

20. Yu, H.; Zou, W.; Chen, J.; Chen, H.; Yu, Z.; Huang, J.; Tang, H.; Wei, X.; Gao, B., Biochar amendment improves crop production in problem soils: A review. *Journal of Environmental Management* **2019,** *232*, 8-21.

21. Suopajärvi, H.; Kemppainen, A.; Haapakangas, J.; Fabritius, T., Extensive review of the opportunities to use biomass-based fuels in iron and steelmaking processes. *Journal of Cleaner Production* **2017,** *148*, 709-734.

22. Wu, Z.; Ma, C.; Jiang, Z.; Luo, Z., Structure evolution and gasification characteristic analysis on co-pyrolysis char from lignocellulosic biomass and two ranks of coal: Effect of wheat straw. *Fuel* **2019,** *239*, 180-190.

23. Mushtaq, F.; Mat, R.; Ani, F. N., A review on microwave assisted pyrolysis of coal and biomass for fuel production. *Renewable and Sustainable Energy Reviews* **2014,** *39*, 555-574.

24. (a) Uebersfeld, J.; ÉTienne, A.; Combrisson, J., Paramagnetic Resonance, a New Property of Coal-like Materials. *Nature* **1954,** *174* (4430), 614-614; (b) Petrakis, L.; Grandy, D. W., Electron spin resonance spectrometric study of free radicals in coals. *Analytical Chemistry* **1978,** *50* (2), 303-308.

25. (a) Petrakis, L.; Grandy, D. W., Free radicals in coal and coal conversions. 6. Effects of liquefaction process variables on the in-situ observation of free radicals. *Fuel* **1981,** *60* (11), 1017-1021; (b) Srinivasan, G.; Seehra, M. S., Effect of pyrite and pyrrhotite on free radical formation in coal. *Fuel* **1983,** *62* (7), 792-794; (c) Sprecher, R. F.; Retcofsky, H. L., Observation of transient free radicals during coal pyrolysis. *Fuel* **1983,** *62* (4), 473-476; (d) Yokono, T.; Obara, T.; Sanada, Y.; Shimomura, S.; Imamura, T., Characterization of carbonization reaction of petroleum residues by means of high-temperature ESR and transferable hydrogen. *Carbon* **1986,** *24* (1), 29-32.

26. (a) Meng, J.; Smirnova, T. I.; Song, X.; Moore, A.; Ren, X.; Kelley, S.; Park, S.; Tilotta, D., Identification of free radicals in pyrolysis oil and their impact on bio-oil stability. *RSC Advances* **2014,** *4* (56), 29840-29846; (b) Trubetskaya, A.; Jensen, P. A.; Jensen, A. D.; Glarborg, P.; Larsen, F. H.; Andersen, M. L., Characterization of free radicals by electron spin resonance spectroscopy in biochars from pyrolysis at high heating rates and at high temperatures. *Biomass and Bioenergy* **2016,** *94*, 117-129.

27. Wu, H.; Quyn, D. M.; Li, C.-Z., Volatilisation and catalytic effects of alkali and alkaline earth metallic species during the pyrolysis and gasification of Victorian brown coal. Part III. The importance of the interactions between volatiles and char at high temperature. *Fuel* **2002,** *81* (8), 1033-1039.

28. Chen, X.; Liu, L.; Zhang, L.; Zhao, Y.; Qiu, P., Pyrolysis Characteristics and Kinetics of Coal–Biomass Blends during Co-Pyrolysis. *Energy & Fuels* **2019,** *33* (2), 1267-1278.

29. Brunauer, S.; Emmett, P. H.; Teller, E., Adsorption of Gases in Multimolecular Layers. *Journal of the American Chemical Society* **1938,** *60* (2), 309-319.

30. Lippens, B. C.; Linsen, B. G.; Boer, J. H. d., Studies on pore systems in catalysts I. The adsorption of nitrogen; apparatus and calculation. *Journal of Catalysis* **1964,** *3* (1), 32-37.

31. Matthews, M. J.; Pimenta, M. A.; Dresselhaus, G.; Dresselhaus, M. S.; Endo, M., Origin of dispersive effects of the Raman D band in carbon materials. *Physical Review B* **1999,** *59* (10), R6585-R6588.

32. Gerson, F., *Electron Spin Resonance Spectroscopy of Organic Radicals*. Wiley-VCH: 2003.

33. Yadav, L., *Organic Spectroscopy*. Springer: 2005.

34. (a) Miura, K., Mild conversion of coal for producing valuable chemicals. *Fuel Processing Technology* **2000,** *62* (2), 119-135; (b) Zhou, Q.; Liu, Q.; Shi, L.; Yan, Y.; Liu, Z., Behaviors of coking and radicals during reaction of volatiles generated from fixed-bed pyrolysis of a lignite and a subbituminous coal. *Fuel Processing Technology* **2017,** *161*, 304-310.

35. Cha, C. Y.; Kim, B. I.; Lumpkin, R. E.; Quinga, E. M. Y., ELECTROMAGNETIC ENHANCEMENT OF CHEMICAL REACTIONS (Devolatilization of Char and Coal). *Fuel Science and Technology International* **1993,** *11* (9), 1175-1202.

36. Hunt, J.; Ferrari, A.; Lita, A.; Crosswhite, M.; Ashley, B.; Stiegman, A. E., Microwave-Specific Enhancement of the Carbon-Carbon Dioxide (Boudouard) Reaction. *Journal of Physical Chemistry C* **2013,** *117* (51), 26871-26880.

37. Motasemi, F.; Afzal, M. T., A review on the microwave-assisted pyrolysis technique. *Renewable & Sustainable Energy Reviews* **2013,** *28*, 317-330.

38. Zhou, F.; Cheng, J.; Liu, J.; Wang, Z.; Zhou, J.; Cen, K., Improving the permittivity of Indonesian lignite with NaCl for the microwave dewatering enhancement of lignite with reduced fractal dimensions. *Fuel* **2015,** *162*, 8-15.

39. Menéndez, J. A.; Domínguez, A.; Fernández, Y.; Pis, J. J., Evidence of Self-Gasification during the Microwave-Induced Pyrolysis of Coffee Hulls. *Energy & Fuels* **2007,** *21* (1), 373-378.

40. Ania, C. O.; Parra, J. B.; Menéndez, J. A.; Pis, J. J., Effect of microwave and conventional regeneration on the microporous and mesoporous network and on the adsorptive capacity of activated carbons. *Microporous and Mesoporous Materials* **2005,** *85* (1–2), 7-15.

41. (a) Hassan, H. M. A.; Abdelsayed, V.; Khder, A. E. R. S.; AbouZeid, K. M.; Terner, J.; El-Shall, M. S.; Al-Resayes, S. I.; El-Azhary, A. A., Microwave synthesis of graphene sheets supporting metal nanocrystals in aqueous and organic media. *Journal of Materials Chemistry* **2009,** *19* (23), 3832-3837; (b) Rosana, M. R.; Hunt, J.; Ferrari, A.; Southworth, T. A.; Tao, Y.; Stiegman, A. E.; Dudley, G. B., Microwave-Specific Acceleration of a Friedel-Crafts Reaction: Evidence for Selective Heating in Homogeneous Solution. *Journal of Organic Chemistry* **2014,** *79* (16), 7437-7450.

42. Benoit, H. H. P. Asphalt composition and method for producing and/or renovating at least one asphalt surface layer. WO2016193082A1, 2016.

43. (a) Takagi, H.; Maruyama, K.; Yoshizawa, N.; Yamada, Y.; Sato, Y., XRD analysis of carbon stacking structure in coal during heat treatment. *Fuel* **2004,** *83* (17–18), 2427-2433; (b) Liu, H.; Xu, L.; Jin, Y.; Fan, B.; Qiao, X.; Yang, Y., Effect of coal rank on structure and dielectric properties of chars. *Fuel* **2015,** *153*, 249-256.

44. (a) Li; Zhuang, Catalytic Reduction of Calcium Sulfate to Calcium Sulfide by Carbon Monoxide. *Industrial & Engineering Chemistry Research* **1999,** *38* (9), 3333-3337; (b) Mu, J.; Zaremba, G., Effect of carbon and silica on the reduction of calcium sulfate. *Thermochimica Acta* **1987,** *114* (2), 389-392.

45. Sheng, C., Char structure characterised by Raman spectroscopy and its correlations with combustion reactivity. *Fuel* **2007,** *86* (15), 2316-2324.

46. (a) Sadezky, A.; Muckenhuber, H.; Grothe, H.; Niessner, R.; Pöschl, U., Raman microspectroscopy of soot and related carbonaceous materials: Spectral analysis and structural information. *Carbon* **2005,** *43* (8), 1731-1742; (b) Beyssac, O.; Goffé, B.; Petitet, J.-P.; Froigneux, E.; Moreau, M.; Rouzaud, J.-N., On the characterization of disordered and heterogeneous carbonaceous materials by Raman spectroscopy. *Spectrochimica Acta Part A: Molecular and Biomolecular Spectroscopy* **2003,** *59* (10), 2267-2276.

47. Li, X.; Hayashi, J.-i.; Li, C.-Z., FT-Raman spectroscopic study of the evolution of char structure during the pyrolysis of a Victorian brown coal. *Fuel* **2006,** *85* (12), 1700-1707.

48. (a) Cuesta, A.; Dhamelincourt, P.; Laureyns, J.; Martínez-Alonso, A.; Tascón, J. M. D., Raman microprobe studies on carbon materials. *Carbon* **1994,** *32* (8), 1523-1532; (b) Jawhari, T.; Roid, A.; Casado, J., Raman spectroscopic characterization of some commercially available carbon black materials. *Carbon* **1995,** *33* (11), 1561-1565.

49. Xu, L.; Liu, H.; Jin, Y.; Fan, B.; Qiao, X.; Jing, B., Structural order and dielectric properties of coal chars. *Fuel* **2014,** *137*, 164-171.

50. Mamaeva, A.; Tahmasebi, A.; Tian, L.; Yu, J., Microwave-assisted catalytic pyrolysis of lignocellulosic biomass for production of phenolic-rich bio-oil. *Bioresource Technology* **2016,** *211*, 382-389.

51. (a) Blesa, M. J.; Miranda, J. L.; Moliner, R.; Izquierdo, M. T.; Palacios, J. M., Low-temperature co-pyrolysis of a low-rank coal and biomass to prepare smokeless fuel briquettes. *Journal of Analytical and Applied Pyrolysis* **2003,** *70* (2), 665-677; (b) Sonobe, T.; Worasuwannarak, N.; Pipatmanomai, S., Synergies in co-pyrolysis of Thai lignite and corncob. *Fuel Processing Technology* **2008,** *89* (12), 1371-1378.

52. Collot, A. G.; Zhuo, Y.; Dugwell, D. R.; Kandiyoti, R., Co-pyrolysis and co-gasification of coal and biomass in bench-scale fixed-bed and fluidised bed reactors. *Fuel* **1999,** *78* (6), 667-679.

53. Yuan, S.; Chen, X.-l.; Li, W.-f.; Liu, H.-f.; Wang, F.-c., Nitrogen conversion under rapid pyrolysis of two types of aquatic biomass and corresponding blends with coal. *Bioresource Technology* **2011,** *102* (21), 10124-10130.

54. (a) Fowler, T. G.; Bartle, K. D.; Kandiyoti, R., Limitations of electron spin resonance spectroscopy in assessing the role of free radicals in the thermal reactions of coal. *Energy & Fuels* **1989,** *3* (4), 515-522; (b) Maskos, Z.; Khachatryan, L.; Cueto, R.; Pryor, W. A.; Dellinger, B., Radicals from the Pyrolysis of Tobacco. *Energy & Fuels* **2005,** *19* (3), 791-799.

55. (a) Delhaes, P.; Marchand, A., Analyse de la forme et de la position de signaix rpe observes sur des carbones graphitiques pulverulents. *Carbon* **1968,** *6* (2), 257-266; (b) Barclay, L. R. C.; Vinqvist, M. R., Membrane peroxidation: Inhibiting effects of water- soluble antioxidants on phospholipids of different charge types. *Free Radical Biology and Medicine* **1994,** *16* (6), 779-788.

56. Fernández, Y.; Arenillas, A.; Díez, M. A.; Pis, J. J.; Menéndez, J. A., Pyrolysis of glycerol over activated carbons for syngas production. *Journal of Analytical and Applied Pyrolysis* **2009,** *84* (2), 145-150.

57. Mok, W. S. L.; Antal, M. J., Effects of pressure on biomass pyrolysis. I. Cellulose pyrolysis products. *Thermochimica Acta* **1983,** *68* (2), 155-164.

58. Bardet, M.; Hediger, S.; Gerbaud, G.; Gambarelli, S.; Jacquot, J. F.; Foray, M. F.; Gadelle, A., Investigation with 13C NMR, EPR and magnetic susceptibility measurements of char residues obtained by pyrolysis of biomass. *Fuel* **2007,** *86* (12), 1966-1976.

59. Green, U.; Aizenshtat, Z.; Ruthstein, S.; Cohen, H., Reducing the spin-spin interaction of stable carbon radicals. *Physical Chemistry Chemical Physics* **2013,** *15* (17), 6182-6184.

60. Wood B J, S. K., Sheridan DR, Chan BL, Wise H *The mechanism of catalytic gasification of coal char*; DE82-009461; US Department of Energy: 1981; pp DE82-009461.

61. (a) Gilman, J. W.; Lomakin, S.; Kashiwagi, T.; VanderHart, D. L.; Nagy, V., Characterization of flame-retarded polymer combustion chars by solid-state 13C and 29Si NMR and EPR. *Fire and Materials* **1998,** *22* (2), 61-67; (b) Butt, D. A. E., Formation of phenols from the low-temperature fast pyrolysis of Radiata pine (Pinus radiata): Part I. Influence of molecular oxygen. *Journal of Analytical and Applied Pyrolysis* **2006,** *76* (1), 38-47; (c) Marsh, H.; Walker, P. L., The effects of impregnation of coal by alkali salts upon carbonization properties. *Fuel Processing Technology* **1979,** *2* (1), 61-75.

62. (a) Knudsen, J. N.; Jensen, P. A.; Dam-Johansen, K., Transformation and Release to the Gas Phase of Cl, K, and S during Combustion of Annual Biomass. *Energy & Fuels* **2004,** *18* (5), 1385-1399; (b) Friebele, E. J.; Griscom, D. L.; Rau, K., Observation of the methyl radical CH3. in irradiated, high-purity synthetic fused silica. *Journal of Non-Crystalline Solids* **1983,** *57* (1), 167-175.

63. Wen, W.-Y., Mechanisms of Alkali Metal Catalysis in the Gasification of Coal, Char, or Graphite. *Catalysis Reviews* **1980,** *22* (1), 1-28.

64. (a) Stewart, I.; Whiteway, S. G.; Cleyle, P. J.; Caley, W. F., Decomposition of Pyrite in a Coal Matrix during the Pyrolysis of Coal. In *Mineral Matter and Ash in Coal*, American Chemical Society: 1986; Vol. 301, pp 485-499; (b) Chen, H.; Li, B.; Zhang, B., Decomposition of pyrite and the interaction of pyrite with coal organic matrix in pyrolysis and hydropyrolysis. *Fuel* **2000,** *79* (13), 1627-1631.

65. (a) Franklin, H. D.; Peters, W. A.; Howard, J. B., Mineral matter effects on the rapid pyrolysis and hydropyrolysis of a bituminous coal. 1. Effects on yields of char, tar and light gaseous volatiles. *Fuel* **1982,** *61* (2), 155-160; (b) Franklin, H. D.; Peters, W. A.; Cariello, F.; Howard, J. B., Effects of calcium minerals on the rapid pyrolysis of a bituminous coal. *Industrial & Engineering Chemistry Process Design and Development* **1981,** *20* (4), 670-674.

66. Tuck, L. D.; Schieser, D. W., ELECTRON SPIN RESONANCE OF SOME NITROGEN-CONTAINING AROMATIC FREE RADICALS1,2. *The Journal of Physical Chemistry* **1962,** *66* (5), 937-939.

67. Trubetskaya, A.; Larsen Andersen, M.; Talbro Barsberg, S., The Nature of Stable Char Radicals: An ESR and DFT Study of Structural and Hydrogen Bonding Requirements. *ChemPlusChem* **2018,** *83* (8), 780-786.

68. Lewis, I. C., Chemistry of carbonization. *Carbon* **1982,** *20* (6), 519-529.